Life Sciences 225 (2019) 117–131

Contents lists available at ScienceDirect

Life Sciences

journal homepage: www.elsevier.com/locate/lifescie

# Osthole attenuates APP-induced Alzheimer's disease through up-regulating miRNA-101a-3p

Ying Lin[1], Xicai Liang[1], Yingjia Yao, Honghe Xiao, Yue Shi, Jingxian Yang*

*Liaoning University of Traditional Chinese Medicine, Dalian, Liaoning 116600, China*

ARTICLE INFO

*Keywords:*
Alzheimer's disease
Osthole
Microarray
MicroRNA-101a-3p
Amyloid precursor protein

ABSTRACT

*Aim:* Alzheimer's disease (AD) is a slowly progressing neurodegenerative disorder that attributed to the increase of amyloid precursor protein (APP). Recently, evidence indicates that microRNA alterations are involved in the development of AD. In this paper, we demonstrated whether osthole could delay the occurrence of AD by regulating miRNA.

*Methods:* Microarray was used to discover differential miRNAs in AD. The target genes regulated by miRNA were predicted by databases; The protective effects of osthole on APP/PS1 mice were determined by Morris Water Maze, H&E and Nissl staining; The APP-SH-SY5Y cells were transfected with miRNA-101a-3p inhibitor, the expression of miRNA-101a-3p and APP mRNA in APP/PS1 mice and APP-SH-SY5Y cells were detected by RT-PCR; And western blot and ICC staining were used to detect the APP and Aβ proteins expression.

*Key findings:* MiRNA-101a-3p was the osthole-mediated miRNA in AD and APP is the target gene. Osthole could increase the learning and memory ability in APP/PS1 mice and inhibit APP mRNA/protein expression by up-regulating miRNA-101a-3p. For exploring the underlying mechanism, miR-101a-3p inhibitor was transfected into the APP-SH-SY5Y cells. We can know that osthole had a protective effect on APP-SH-SY5Y cells, and it could raise miRNA-101a-3p expression and inhibit APP mRNA/protein expression, the formation of Aβ protein was inhibited too.

*Significance:* These results emphasized that osthole had a protective effect on APP/PS1 mice and APP-SH-SY5Y cells. The main cause was due to osthole could inhibit APP expression by up-regulating miRNA-101a-3p so as to help delay the occurrence of AD.

## 1. Introduction

Alzheimer's disease (AD) is an age-related condition which presents in three forms. The most common type is dementia [1–3]. Various hypotheses have been described in relation to the pathogenesis of AD. Currently, the most widely accepted hypothesis is amyloid-β peptide (Aβ) deposition [4–6]. This is one of the cleaved by-products of the amyloid precursor protein (APP) by β-secretase [7–9]. Aβ accumulates and forms Aβ plaque when the levels of APP are increased in the brain. So, it would be an effective method to delay the occurrence of AD by inhibiting the expression of APP then reducing the formation of additional neurotoxic substance.

Osthole (C15H16O3), a bioactive component derived from the traditional Chinese medicine [10–12], has diverse pharmacological effects, such as anti-inflammatory, anti-apoptosis, anti-oxidative stress [13]. It is reported that osthole could prevent ALCL3-induced Alzheimer's disease in mice [14], and the PI3K/AKT signaling pathway was one of the osthole-regulated pathways in Alzheimer's disease ([15]).

MicroRNAs (miRNA), a class of non-coding RNAs, regulated numerous Physiological processes [16–18] via binding to the 3′ untranslatable region (3′-UTR) of their mRNA targets. Aberrant expression of microRNAs in the brain maybe a hall marker of some diseases, Hui Che [19] investigated that miR-101 was higher in younger rats than middle-aged rats. And APP was a target gene regulated by miR-101 [20]. So, we explore whether or not osthole had the effects on the miRNAs expression and then influenced the occurrence of AD by regulating the target genes.

Previous study of our laboratory found that osthole not only suppressed the expression of BACE-1 by up-regulating miR-107 [21], also inhibited the expression of CAMKK2 and its downstream p-AMPKα via up-regulating miR-9 [22,23]. In this study, APP/PS1 mice who divided

* Corresponding author.
*E-mail address:* jingxianyang@yahoo.com (J. Yang).
[1] These authors contributed equally to this work.

https://doi.org/10.1016/j.lfs.2019.04.004
Received 12 December 2018; Received in revised form 24 March 2019; Accepted 1 April 2019
Available online 03 April 2019
0024-3205/ 

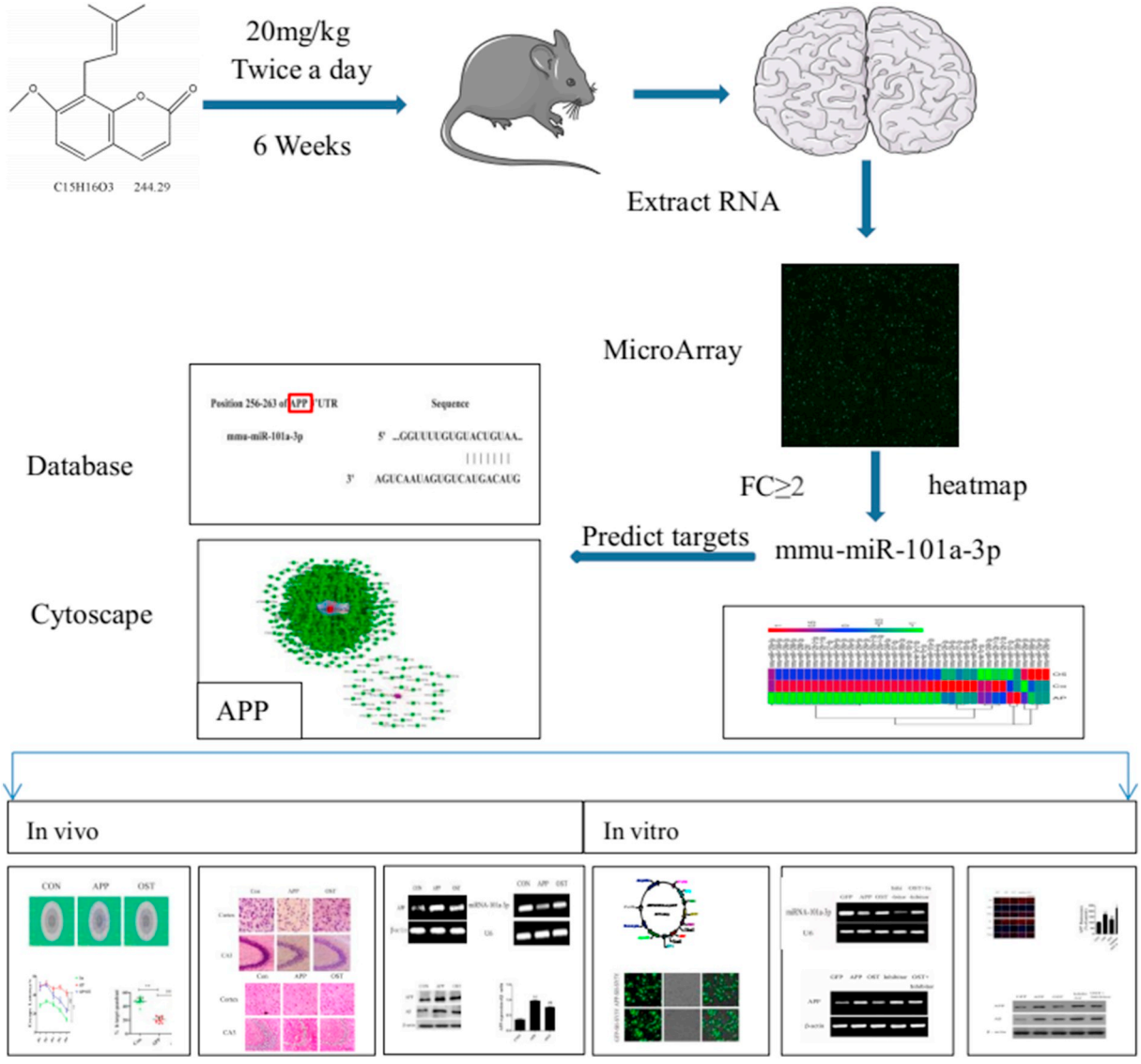


**Fig 1.** The whole framework for exploring the relationship between miR-101a-3p and APP in Alzheimer's disease.

into APP, and osthole group were used to discover the osthole-mediated miRNAs determined by microarray, then miR-101a-3p was selected as the osthole-mediated miRNA and the result that miR-101a-3p has a negative correlation with APP was verified by databases and cytoscape3.6.1. These findings suggested that miR-101a-3p may be a therapeutic target for treating Alzheimer's disease. Here, we extended this investigation and asked whether osthole up-regulate miR-101a-3p along with the reduction of the involved gene expression. First, SH-SY5Y cells which stably infected with the human Swedish-type mutated APP and APP/Presenilin 1 [PS1] double transgenic mice were the models in vitro and vivo respectively. The present study was design to find osthole-regulated miRNAs which block the development of AD to further study the possible mechanism of osthole in AD and open up a new way for the treatment of AD.

## 2. Materials and methods

### 2.1. Animals and osthole treatment

160 mg osthole ($C_{15}H_{16}O_3$, > 98% purity; obtained from the National Institute for the Control of Pharmaceutical and Biological products; 110822-200407; Beijing, China) was dissolved in 80 mL 0.05% Sodium carboxymethyl cellulose (CMC-Na, C = 20 mg/kg) and store at 4 °C [24].

APP/PS1 double transgenic mice (9 months; from the Institute of Zoology, Nanjing University) which expressed the APP and PS1 genes were raised in the room (23 ± 1 °C). The food and water were free access. APP/PS1 mice [25,26] served as APP group ($N$ = 10). Osthole group was the APP/PS1 mice with osthole 20 mg/kg administration, twice a day for 6 weeks. C57BL/6 mice (Liaoning Changsheng Biotechnology Co., Ltd. $N$ = 10) were used as control group. APP and the control group were given equivalent amount of 0.05% CMC-Na.

### 2.2. Morris Water Maze and data analysis

The spatial learning and memory performance were detected by Morris Water Maze (MWM, Chengdu TME Technology Co., Ltd., Chengdu, China) with blind method. Briefly, Water was dyed white with milk in advance and kept at 21 °C. The escape platform was hidden below two centimeters depth of the surface of water in the target

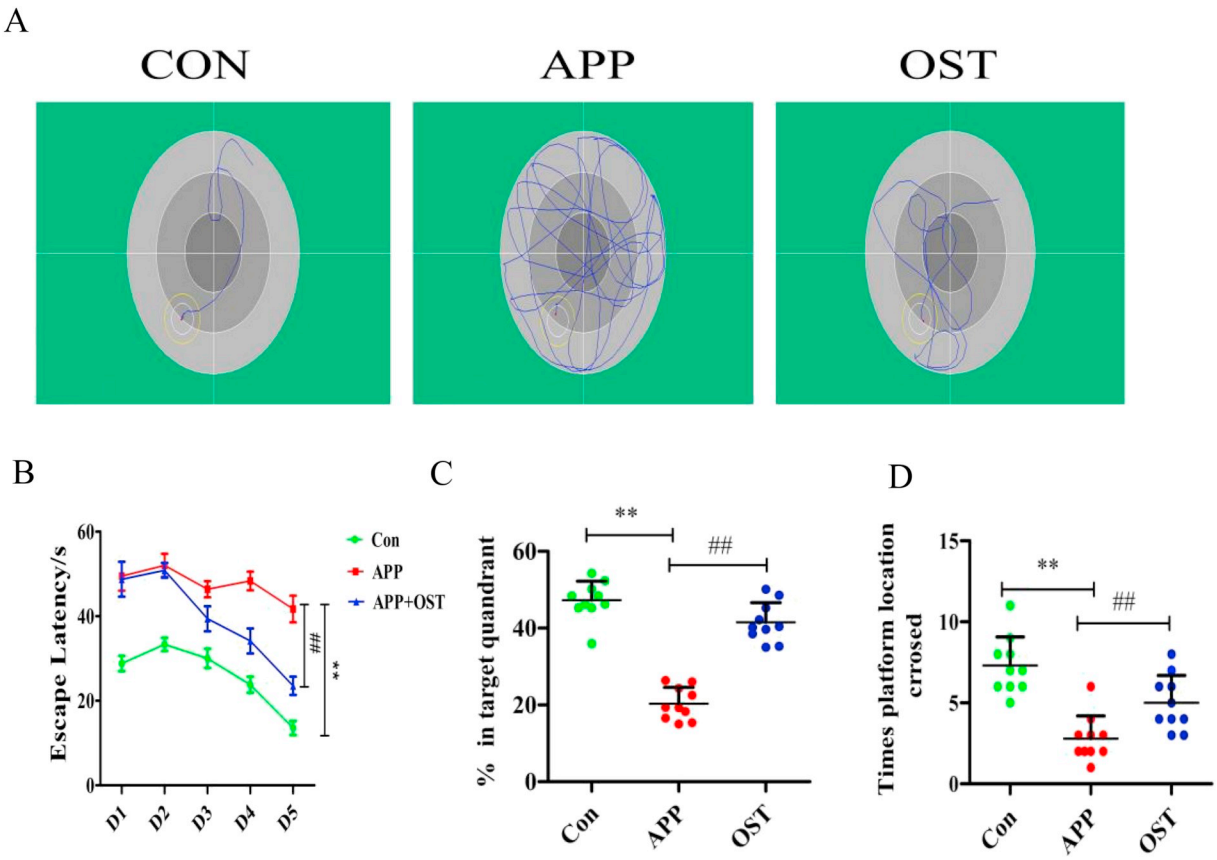


**Fig. 2.** Osthole enhances the learning and memory ability in APP/PS1 mice
(A) Representative individual swim paths in the water maze trial (on day 5).
(B) The escape latency in the 5 day's experiments of the water maze task.
(C) The percentage of distance spent in the correct quadrant.
(D) The number of times the platform location was crossed. $^{**}P < 0.01$ vs. CON; $^{\#\#}P < 0.01$ vs. APP; values are expressed as the mean ± SD ($n = 10$). (D) is expressed as the median ± IQR ($n = 10$).

quadrant. Mice were placed into four quadrants respectively. The escape latency, platform quadrant distance and crossing platform times were monitored by the video analysis system and compared [25,26]. At last, the differences were determined by *t*-test.

### 2.3. H&E and Nissl staining

After MWM test, all groups of animals were sacrificed and the brains were harvested for pathological and immunological assessment. The mouse brain was embedded in Tissue-Tek (SAKURA) and frozen in a refrigerator at −80. The hippocampus was sliced to 7 μm using a cryostat (CM1900, Leica). The H&E staining process was as follow: The sections were stained with 70%, 80%, 90% alcohol (5 s), 50 °C hematoxylin (30 s), 1% hydrochloric acid (5 s), 0.5% ammonia (10 s), and eosin (5 s), 70%, 80%, 90% alcohol (5 s), and finally sealed with neutral gum. The histopathological damage was observed under a microscope [27]. The Nissl staining process was as follow: 100% ethanol (20 s), distilled water (30 s), Cresyl violet (37 °C, 20 min), neutral differentiation solution (30 s), 100% ethanol (20 s), xylene (10 s). The results of H &E and Nissl section were visualized by OLYMPUS SZX9 and BX51 microscope (Tokyo, Japan) with a digital camera.

### 2.4. Microarray analysis

The samples were carried out by Shanghai Ouyi Biomedical Technology Co., Ltd. using Agilent Mouse miRNA, Release 21.0. The total RNA extracted from frozen brain of each group which analyzed by NanoDrop ND-2000 (Thermo Scientific) and Agilent Bioanalyzer 2100 (Agilent Technologies). Finally, the differences expressed among miRNAs were selected using fold changes (FC) ≥ 2 as a standard. The miRNAs with differential expression in each group were demonstrated by heat map.

### 2.5. Bioinformatics analysis of microRNA

The differently expressed miRNA was selected according to the fold changes and heat map, then the target gene regulated by miRNA was predicted by the databases. Owing to the inherent relationship, the results of different databases were combined, including Targetscan [27] (http://www.targetscan.org/vert_72/), miRDB [28] (http://www.mirdb.org/), miRWalk (http://zmf.umm.uni-heidelberg.de/apps/zmf/mirwalk2/), miRsystem (http://mirsystem.cgm.ntu.edu.tw/). At the same time, the network of miR-101a-3p was established to visualize the

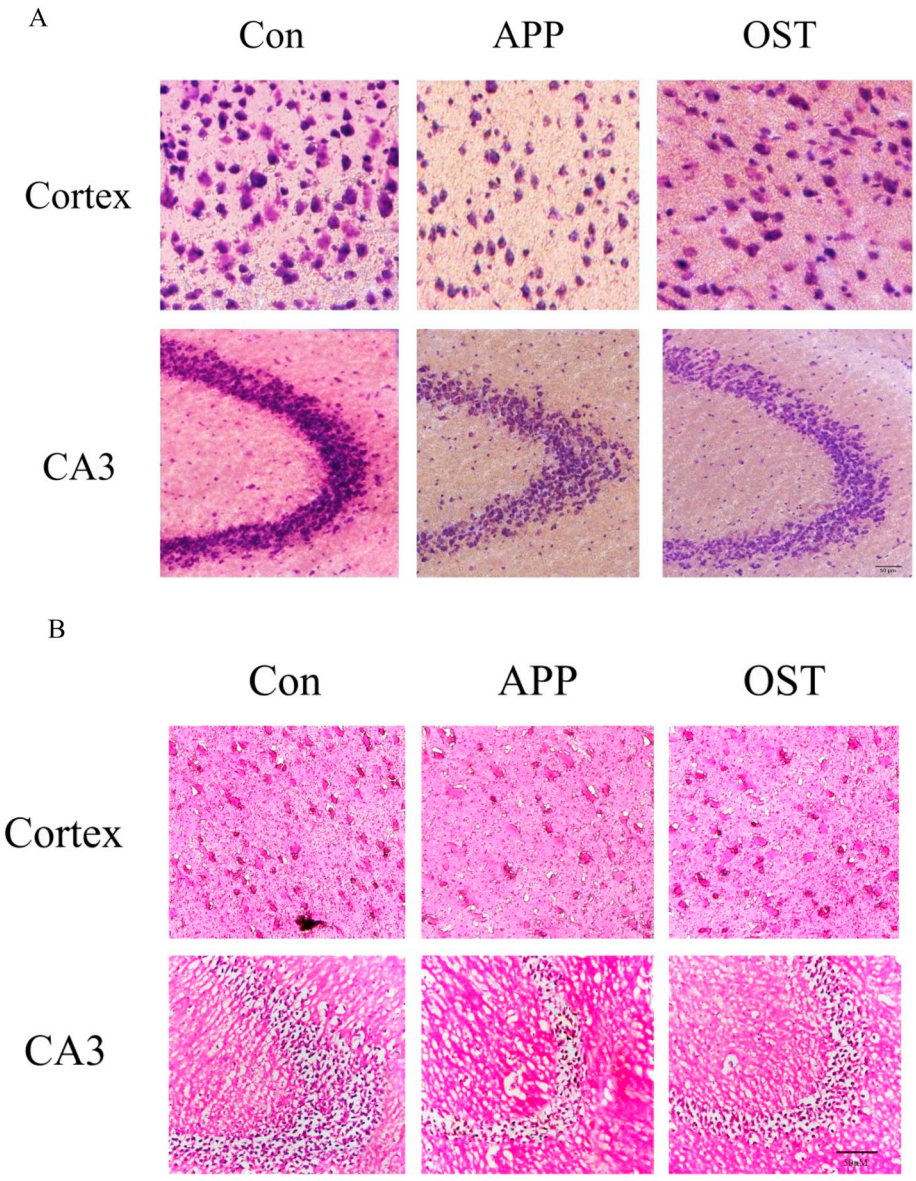


**Fig. 3.** Osthole repair the Pathological damage in hippocampus of APP/PS1 mice determined by Nissl and H&E staining.
(A) Nissl staining of hippocampus and cerebral cortex in three groups of mice;
(B) H&E staining of hippocampus and cerebral cortex of three groups of mice.

regulatory relationships between miRNA and the genes using Cytoscape 3.6.1 [29].

### 2.6. Virus preparation and lentiviral transduction

293T cells were seeded at a density of $2.0 \times 10^5$ cells/mL, GFP or GFP-APP595/596 vector plasmid, pLP1, pLP2, pLP/VSV-G plasmid (Tianjin Medical University) were added into 250 μL DMEM and incubated for 5 min. Lipofectamine 2000 (Thermo Fisher Scientific) and 250 μL DMEM were co-cultured for 5 min at room temperature. Then the products were added into 293T cells and the supernatant was collected after 24, 48, and 72 h to determine the titer by fluorescence intensity. Lentiviral and 1% polybrene were added into SH-SY5Y cells, the expression of APP gene and protein in SH-SY5Y cells were detected by RT-PCR and Western Blot three days later [21], The lentivirus–GFP group was used as control [30,31].

### 2.7. Cell viability

The SH-SY5Y cells were infected with GFP or GFP-APP595/596 Lentivirus, the cells were divided into 3 group, (1) GFP group (infect GFP), (2) APP group (infect APP), (3) OST group (infect APP + various

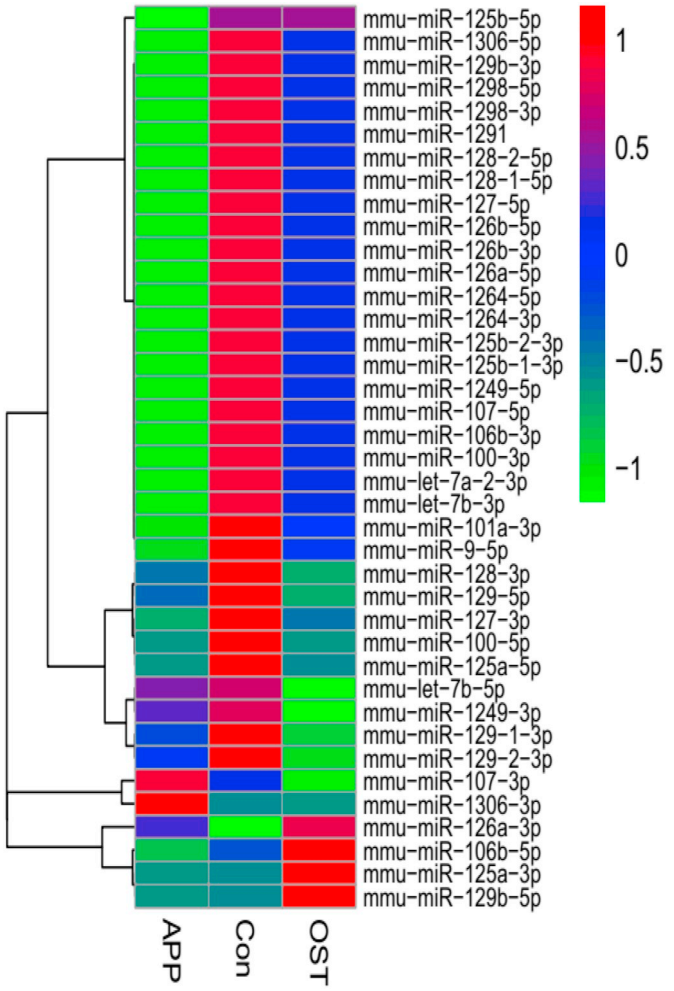


**Fig. 4.** The microRNAs expressed differentially determined by microarray. Green stands for the low expression of miRNA and red stands for over-expression of miRNA; (For interpretation of the references to color in this figure legend, the reader is referred to the web version of this article.)

concentrations of osthole 25, 50, 75, 100 μM). Cells were seeded at a density of $2.0 \times 10^5$ cells/mL. After co-culture for 24 h, 3-(4,5-dimethylthiazol-2-yl)-2,5-diphenylltetra-zolium bromide (MTT, Sigma) was added and incubated for 4 h in the humidified atmosphere of 95% air and 5% CO2, 100 μL of dimethylsulfoxide (DMSO) was added at last. The optical density (OD) value determined by microplate reader (Thermo Fisher Scientific Inc., U.S.A.) at 580 nm were used to reflect the levels of MTT.

### 2.8. Measurement of lactate dehydrogenase (LDH) release

Cells were seeded into 96-well plate at a density of $5 \times 10^3$/well with 100 μL complete medium per well. After the pre-protection of osthole, the Lactate dehydrogenase assay kit (Nanjing Jiancheng Bioengineering Institute) was conducted in accordance with the manufacturer's instructions [32], The optical density (OD) value determined by microplate reader (Thermo Fisher Scientific Inc., U.S.A.) at 490 nm were used to deserve the release of LDH. LDH release represents the extent of cell damage, and all data were repeated three times independently.

### 2.9. MiR-101a-3p inhibitor transfection

MiR-101a-3p inhibitor oligonucleotide (RiboBio, 20 μM) was transfected into cells using Lipofectamine 2000 (5 μL) in 6 well plate, it is the inhibitor group. The cells was divided 5 groups, the establishment of GFP group and APP group were depicted as the method 2.8; OST group (APP + OST 50 μM); Inhibitor group (APP + miR-101a-3p Inhibitor); OST + Inhibitor group (APP + Inhibitor + OST 50 μM). Cells were prepared for the following experiments.

### 2.10. RT-PCR analysis

In this section, we examined the expression of miRNA-101a-3p and its downstream target APP mRNA. The total RNA was isolated from mice brains and SH-SY5Y cells using TRizol reagent (Invitrogen), cells were grouped according to Method 2.10 and converted cDNA by OneScript Reverse Transcriptase OneScript cDNA Synthesis Kit (Abm). The microRNA reverse transcription was performed using bulge-loop TM miRNA reverse primer instead of Olige (dT). 25 μL Dream Taq PCR Master Mix (Abm), 1.5 μL forward and reverse primer (RiboBio, Guangzhou), 2 μL cDNA and 20 μL water nuclease free in amplification reaction mixture (50 μL), and the PCR condition were as follows: 95 °C (2 min, a cycle), 95 °C (30 s), 58 °C (30 s), 72 °C (1 min), 35 cycles in total. Finally, 72 °C (10 min, a cycle). β-Actin served as the control of APP and U6 snRNA (U6) served as control of miR-101a-3p, the primer sequence was as follows: APP, F: AAAACGAAGTTGAGCCTGTTGAT; R: GAACCTGGTCGAGTGGTCAGT; β-actin, F: TGCTGTCCCTGTATGCC TCT; R: TTTGATGTCACGCACGATTT. Primer of miRNA-101a-3p was designed by RiboBio (Guangzhou, China).

### 2.11. ICC staining

The cells are grouped according to Method 2.10 for ICC staining. The cells were fixed with 4% paraformaldehyde then permeabilized by 1% Triton X-100. The APP and Aβ primary antibodies (1:400, Bioss) were added to the cells of each group afterwards and incubated at 4 °C overnight. The next morning, goat anti-rabbit secondary antibodies (1:1000; Jackson, West Grove, PA, USA) were co-cultured with the cells at room temperature for 1 h. DAPI and anti-fluorescence quencher were added. It's necessary to wash with PBS three times between each step. The fluorescence intensity of photographs was checked under a microscope, and quantitative analysis of fluorescence intensity was performed using ImageJ software.

### 2.12. Western blot

The total proteins of the cells and mice were extracted with readyPrep protein extraction kit. Protein quantification was determined by BCA protein assay (Shenyang WanLei Biological Technology Co., Ltd.). 50 μg total protein from each samples were loaded on 10% SDS-PAGE and transferred to polyvinylidene difluoride (PVDF) membrane using a wet transfer system (Bio-Rad, USA). APP (1:400, Bioss) and Aβ (1:500, Shenyang Wanlei Biological Technology Co., Ltd.) primary antibodies. Appropriate HRP Goat Anti-Rabbit lgG secondary antibodies (1:2000, ABclonal Technology) were used to incubate to the

membranes. At last, ImageJ software was used to identify the protein quantification.

### 2.13. Statistical analysis

All data were analyzed by SPSS version 13.0 (SPSS, IL, USA) and graphs were drawn by GraphPad Prim 5.0 software. The normal distribution of the data was detected by Box plot. The data conforming to the normal distribution was expressed as mean ± standard deviation (mean ± SD), and the comparison between groups was analyzed by variance, and the *t*-test was used for comparison between the two groups. $P < 0.05$ was considered statistically significant.

## 3. Results

The molecular mechanism of osthole in AD was visualized by a whole framework with the experiment procedure based on pharmacological data (Fig. 1).

### 3.1. Osthole increases the learning and memory ability of APP/PS1 mice

The effects of osthole on the learning and memory ability in APP/PS1 mice were evaluated by Water Morris Maze. The swimming distance is shortest in control group and shortened significantly with the treatment of osthole compared with APP group (Fig. 2A). And the statistical data of escape latency showed that the APP/PS1 mice with osthole treatment found the platform quicker than APP group (OST group: $N = 10$, 32.767 ± 1.893% vs. 20.933 ± 2.532%. vs. APP group. $P < 0.01$). The escape latency reduced gradually with the training of MWM (Fig. 2B), but there was no significant difference in swimming speed between each group of mice (the data was not shown). When we analyzed the distance percentage that the mice swimming in platform quadrant (Fig. 2C), we found that the percentage swimming distance in target quadrant in OST group was increased compared with APP group (OST group: $N = 10$, 29.977 ± 1.295% vs. 12.727 ± 0.735%, vs. APP group, $P < 0.01$). After the 4 days training, similar results were obtained when the crossing platform times was determined (Fig. 2D), the mice with osthole treatment crossed the platform multiple times (OST group: $N = 10$, 5 ± 2 vs. 3 ± 1, vs. APP group, $P < 0.01$). All data indicated that osthole raise the learning and memory ability of APP/PS1 mice.

### 3.2. Osthole repairs the pathological damage in APP/PS1 mice

To investigate the effects of osthole on pathological damage in APP/PS1 mice, H&E and Nissl staining were used. The results of Nissl staining suggested that Nissl bodies were lost, Neuronal atrophy, nuclear contraction and other phenomena have been produced in APP group. In contrast to APP group (Fig. 3A), the numbers of Nissl bodies increased in the hippocampal CA3 region and cerebral cortex of APP/PS1 mice with osthole administration. It can be seen from the results of H&E staining (Fig. 3B) that the cells in the CA3 region and cerebral cortex of the control group were uniform in size and round, while cells and voids cell shrinkage had larger differences in APP group. The structure of the hippocampal CA3 area and cerebral cortex of mice after osthole treatment was improved significantly. It indicated that osthole reduce the Pathological damage of APP/PS1 mice.

A

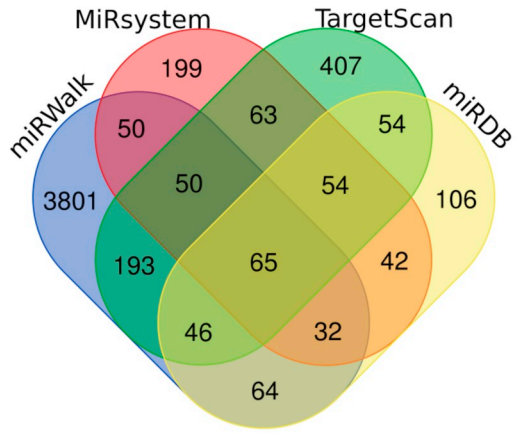


B

| Position 256-263 of APP 3'UTR | | Sequence |
|---|---|---|
| mmu-miR-101a-3p | 5' | ...GGUUUUGUGUACUGUAA... |
| | | \| \| \| \| \| \| \| |
| APP | 3' | AGUCAAUAGUGUCAUGACAUG |

**Fig. 5.** miR-101a-3p could bind to the 3′-UTR of APP.
(A) The Veen chart of miRWalk, TargetScan, miRDB, miRsystem;
(B) The complementary paired sequence which determined by databases;
(C) The validation of APP-related miRNAs by Cytoscape.

C

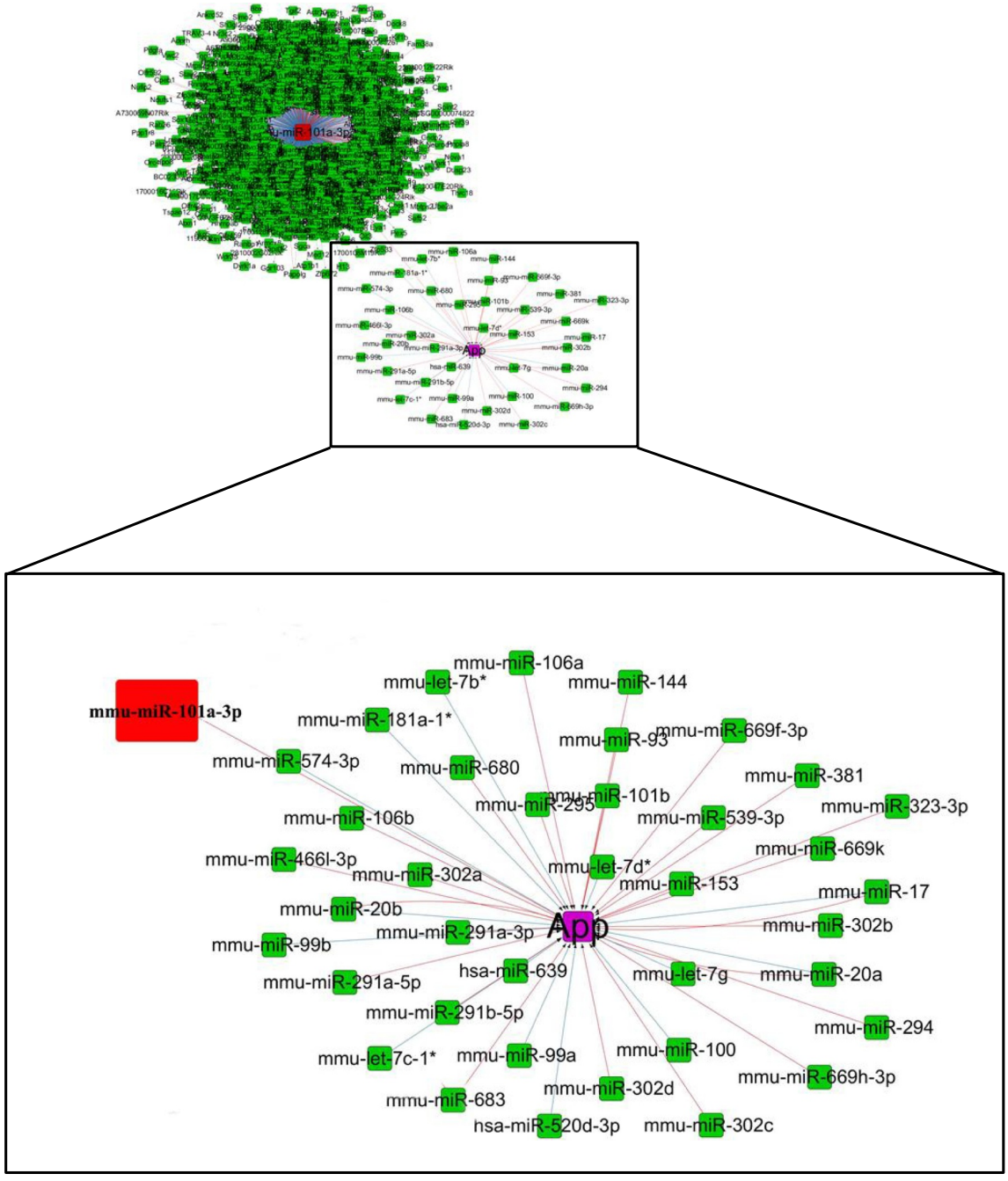


**Fig. 5.** (*continued*)

### *3.3. MiRNA-101a-3p regulated by osthole in APP/PS1 mice*

The Agilent miRNA microarray was used to explore the osthole-regulated microRNAs in APP/PS1 mice, the number of miRNAs expressed differentially in APP/PS1 mice was 111, of which 71 were up-regulated and 40 were down-regulated. The number of miRNAs expressed differentially was 78 with osthole treatment, of which 25 were up-regulated and 53 were down-regulated compared with APP group. The different expression of miR-101a-3p in each group was shown by heat map (Fig. 4), the expression of miR-101a-3p decreased in APP

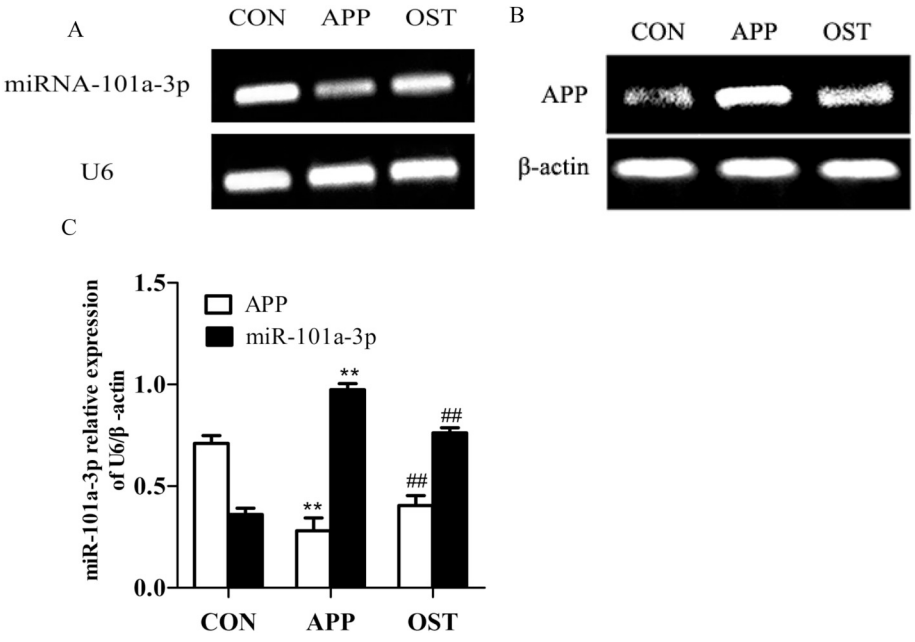


**Fig. 6.** The expression of miRNA-101a-3p and APP with osthole treatment in APP/PS1 mice.
(A, B) The expression of miRNA-101a-3p and APP were analyzed by RT-PCR;
(C) The expression levels were semi-quantified by densitometric measurements, normalized with U6/β-actin internal control; $^{**}P < 0.01$ vs. CON; $^{\#\#}P < 0.01$ vs. APP.

group compared with control group, while increased with the osthole treatment, the differences among the three groups were obvious. So miRNA-101a-3p was chosen for follow-up research.

### 3.4. miR-101a-3p binds to APP gene

To look for the target genes of miRNA-101a-3p, the prediction results of multiple databases were combined, the target genes shared by the four databases are shown by the Venn plot (Fig. 5A), there are 65 genes in four databases, including APP, Atrx, Btbd3, Metap1, Zfhx4 and so on. The complementary paired sequence which determined by databases were shown in Fig. 5B. We know that miRNA-101a-3p had a binding site with the 3′-UTR of APP. At the same time, the miRNAs which was regulated the expression of APP was predicted by Cytoscape3.6.1 (Fig. 5C). Including miR-101a-3p, miR-100, miR-153 and so on. At last, we verified the predicted results from bioinformatics analysis through the experiments in vitro and in vivo.

### 3.5. Osthole regulates the expression of miR-101a-3p and APP mRNA in APP/PS1 mice

To validate the results from Microarray analysis, RT-PCR was used to identify the expression of miR-101a-3p and APP mRNA. Total RNA was extracted from hippocampus and cortex of mice, the products were electrophoresed (Fig. 6A, B). From the statistical graph (Fig. 6C), it can be seen that the relative expression of miRNA-101a-3p in the APP group was decreased (APP group: $N = 6$, 0.281 ± 0.063% vs. 0.710 ± 0.038%, vs. Control group, $P < 0.01$). And the expression of miRNA-101a-3p in osthole group increased significantly (OST group: $N = 6$, 0.405 ± 0.049% vs. 0.281 ± 0.063%, compared with APP group, $P < 0.01$). It can be seen that the APP gene increased significantly in APP group (APP group: $N = 6$, 0.974 ± 0.03% vs. 0.360 ± 0.031%, vs. Con group, $P < 0.01$), while the levels of APP decreased with the treatment of osthole (OST group: $N = 6$, 0.761 ± 0.025% vs. 0.974 ± 0.03%, vs. APP group, $P < 0.01$). We can know that osthole could up-regulated miRNA-101a-3p and reduce the expression of APP gene. The results of the RT-PCR were consistent with those of the microarray and the bioinformatics predicted relationship between miRNA-101a-3p, APP was also verified preliminarily.

### 3.6. Osthole inhibits the expression of APP protein in APP/PS1 mice

We investigated whether or not the expression of APP protein is changed with the osthole treatment. The expression of APP, Aβ proteins in hippocampus and cortex of three groups were detected by Western Blot (Fig. 7A). The results showed that the expression of APP protein in APP group was significantly higher than that in control group (APP group: $N = 6$, 0.991 ± 0.031% vs. 0.377 ± 0.051%, vs. control group, $P < 0.01$). However, the expression of APP protein decreased in osthole group (OST group: $N = 6$, 0.629 ± 0.073% vs. 0.991 ± 0.031%, vs. APP group, $P < 0.01$, Fig. 7B). At the same time, we also detected the changes of Aβ protein, we found that the expression of Aβ protein in OST group was also reduced relatively (OST group: $N = 6$, 0.268 ± 0.059% vs. 0.889 ± 0.042%, vs. APP group, $P < 0.01$). The tendency of Aβ protein is consistent with APP protein. The results indicated that osthole can decrease the expression of APP and Aβ proteins in APP/PS1 mice.

### 3.7. SH-SY5Y cells with over expression of APP was established successfully

As shown in Fig. 8A, it is the schematic diagram of the plasmid structure of APP595/596. APP and the viral vector were double-digested by *Xba*I and *Not*I respectively, then they were reconnected into loop by ligase to form APP595/596 plasmid. The GFP gene which took along green fluorescence was inserted into APP as a fluorescent marker,

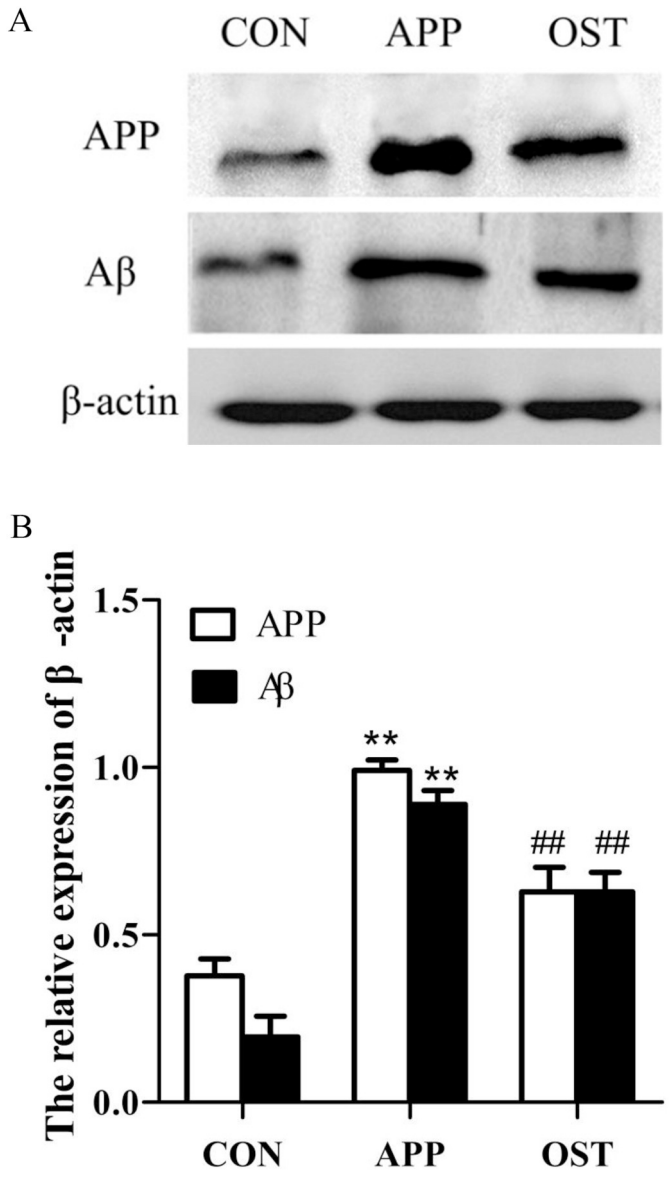


**Fig. 7.** The expression of APP and Aβ proteins with Osthole treatment in APP/PS1 mice.
(A) The expression of APP and Aβ proteins were analyzed by Western blot;
(B) The expression levels were semi-quantified by densitometric measurements, normalized with β-actin internal control. $n = 10$, $^{**}P < 0.01$ vs. CON; $^{\#\#}P < 0.01$, $^{\#}P < 0.05$ vs. APP.

we determined the intensity of fluorescent label to judge if APP plasmid which co-expression GFP plasmid can be transfected into 293T cells successfully. Lentivirus was packaged in 293 cells and infected the SH-SY5Y cells to establish the SH-SY5Y cells with over-expression of APP (APP-SY5Y cells). The green fluorescence of cells was observed under the microscope. As shown in Fig. 8B, the growth tendency of the cells which infect APP was slow. The GFP and APP group were reflect green fluorescence. After three days of culture, the cells were identified by RT-PCR and Western blot (Fig. 8C). It was found that the expression of APP mRNA and protein in APP group were higher compared with GFP group (APP mRNA: 0.160 ± 0.010% vs. 0.030 ± 0.006%; APP protein: 0.866 ± 0.042% vs. 0.436 ± 0.023%, vs. GFP group, $P < 0.01$. Fig. 8D). It suggested that the AD cell model was constructed successfully.

### 3.8. Osthole increases the viability of APP-SY5Y cells

The MTT and LDH kits were used to determine the neuroprotective effects of osthole. We chose the osthole concentrations of 25, 50, 75 and 100 μM to intervene in APP-AY5Y cells. The viability was higher when osthole was at concentrations of 50 and 75 μM (Fig. 9A). However, the precipitation of the drug was occurred at a concentration of 75 μM. The final concentration of osthole in the follow-up test was set to 50 μM. The LDH kit was used to detect the effects of osthole on cell damage, the LDH release was highest in the APP group (166.06 ± 6.11). And the release of LDH in osthole group (134.667 ± 5.005) was between APP and GFP group (100.0 ± 5.001). The results indicated that osthole increase the cell viability and reduce cell damage (Fig. 9B).

### 3.9. Osthole inhibits the expression of APP mRNA by up-regulating miRNA-101a-3p

To investigate the molecular mechanism of osthole in AD whether or not affect the expression of APP by regulating miRNA-101a-3p, miRNA-101a-3p inhibitor (Suzhou Jima Gene Co., Ltd.) was transfected into the cell with over-expression of APP to inhibit the expression of miR-101a-3p.

The total RNA was inverted into cDNA and amplificated (Fig. 10A). As shown in Fig. 10C. It be seen that the inhibitor inhibits the expression of miRNA-101a-3p successfully (0.363 ± 0.05%), miRNA-101a-3p decreased significantly in APP group compared with the GFP group (APP group: 0.645 ± 0.068% vs. 0.963 ± 0.02%, vs. GFP group, $P < 0.01$). The expression of miRNA-101a-3p was decrease in APP group, and increased in the OST group (0.903 ± 0.016%). Next, we determined the expression of APP in each group (Fig. 10B), the expression of APP mRNA was significantly decreased in OST group compared with APP group (OST group: 0.557 ± 0.062% vs. 0.658 ± 0.018%, vs. APP group). And the expression of APP was highest in Inhibitor group (0.726 ± 0.017%), the expression of APP mRNA in OST + Inhibitor group (0.621 ± 0.053%) was between that in OST group and Inhibitor group (Fig. 10C), and the difference was statistically significant ($P < 0.01$).

### 3.10. Osthole inhibits the expression of APP protein in APP-SY5Y cells

In order to prove osthole affects the expression of APP protein through regulating miRNA-101a-3p, Western Blot (Fig. 12) and Immunofluorescence chemistry (Fig. 11A, B) were used. The expression of APP protein was significantly increased in APP group compared with the GFP group (Fig. 11A: 0.739 ± 0.031% vs. 0.31 ± 0.042%, vs. GFP; Fig. 11B: 171.833 ± 8.944 vs. 102.04 ± 3.46 vs. GFP). Compared with APP group, the expression of APP protein was decreased significantly with osthole treatment (Fig. 11A: 0.458 ± 0.033%; Fig. 11B: 126.973 ± 7.178), and the expression of APP protein was the highest in the inhibitor group (Fig. 11A: 0.950 ± 0.043%; Fig. 11B: 227.379 ± 5.671). The co-treatment group (Fig. 11A:

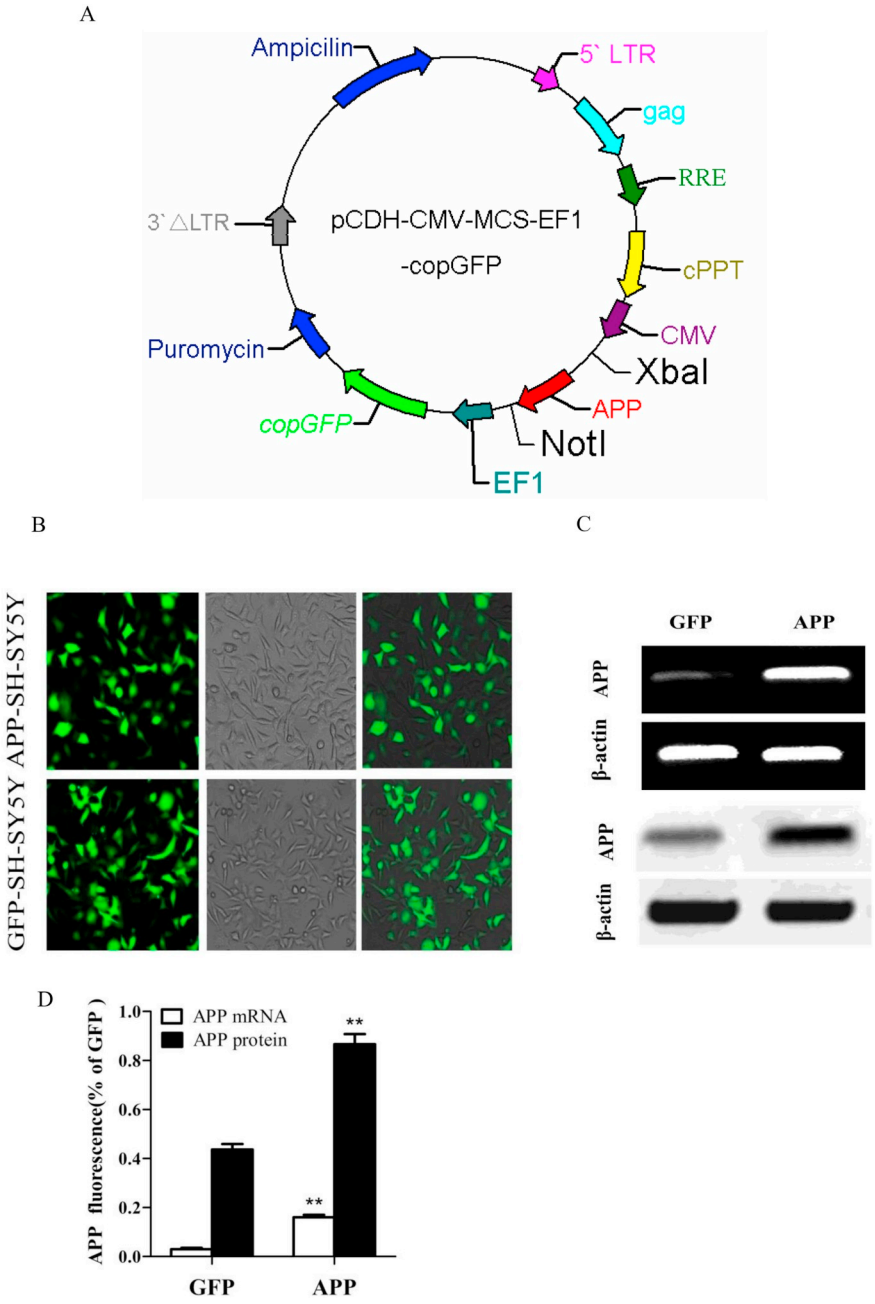


**Fig. 8.** The establishment of SH-SY5Y with over expression of APP.
(A) The structural formula of APP595/596 plasmid;
(B) Green fluorescent cell diagram with APP and GFP plasmid (scale = 50 μm);
(C) The electrophoretic diagram determined by RT-PCR and Western blot;
(D) The expression levels were semi-quantified by densitometric measurements, normalized with β-actin internal control; $^{**}P < 0.01$ vs. GFP.

0.637 ± 0.044%; Fig. 11B: 160.463 ± 9.498) was between osthole group and the inhibitor group, and the difference was statistically significant ($P < 0.01$). MiRNA-101a-3p inhibitor attenuates the inhibitory effect of miR-101a-3p on APP protein expression in APP-SY5Y cells (Fig. 12). And because of the inhibition of APP by MiRNA-101a-3p, the expression of Aβ (1.004 ± 0.052, 216.712 ± 15.974) is decreased at the same time. As shown in Fig. 13, the expression of APP protein is positively correlated with Aβ protein, while the expression of miRNA-

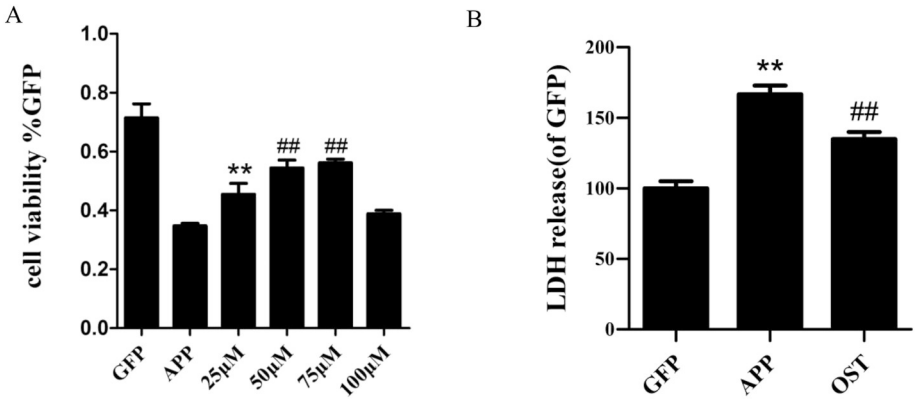


**Fig. 9.** The protective effect of osthole on SH-SY5Y with over-expression of APP.
(A) Cell viability determined by MTT assay;
(B) Cell damage determined by LDH assay;
$^{**}P < 0.01$ vs. GFP; $^{\#\#}P < 0.01$ vs. APP.

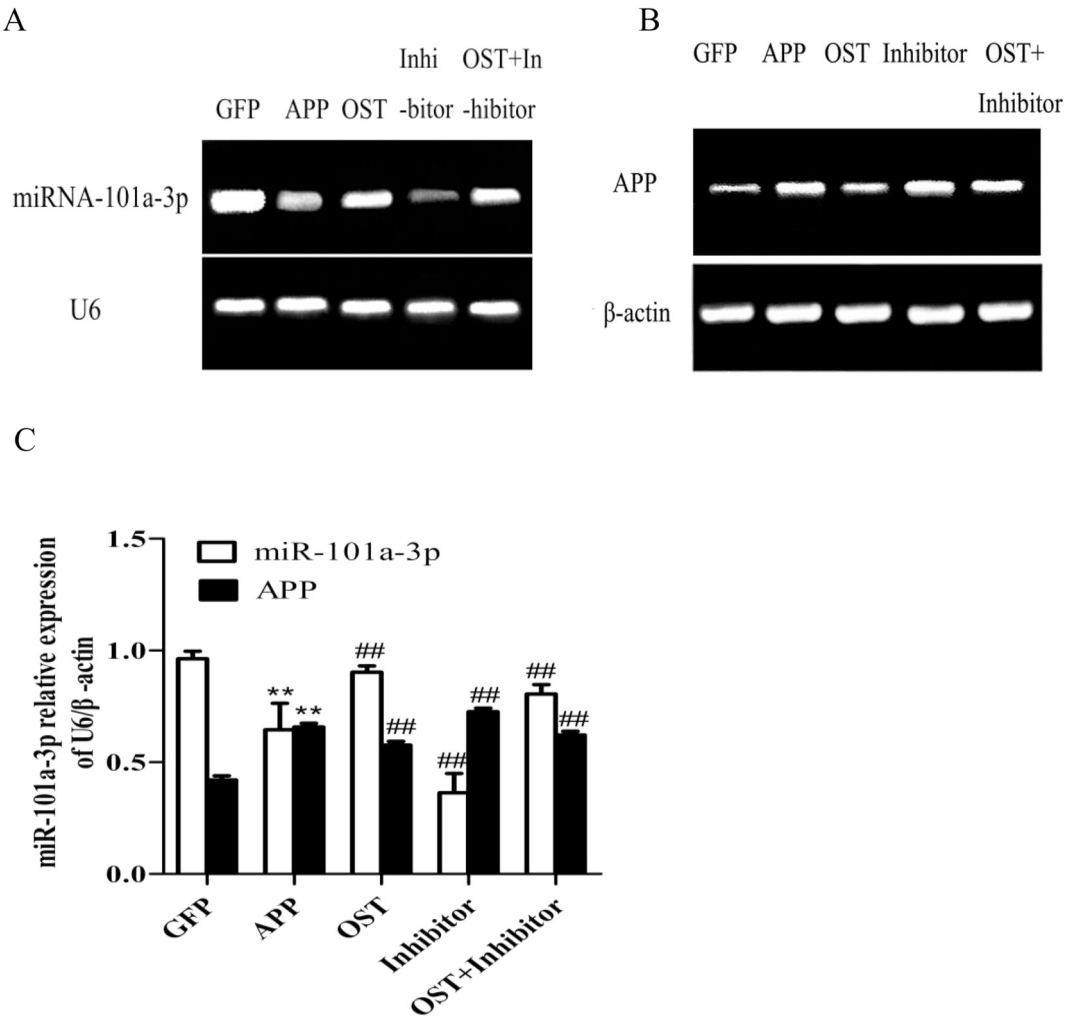


**Fig. 10.** The expression of miRNA-101a-3p and APP with osthole treatment.
(A) The expression of miRNA-101a-3p was analyzed by RT-PCR in APP-SY5Y cells;
(B) The expression of APP was analyzed by RT-PCR in APP-SY5Y cells;
(C) The expression levels were semi-quantified by densitometric measurements, normalized with β-actin internal control;
$^{**}P < 0.01$ vs. GFP; $^{\#\#}P < 0.01$; vs. APP.

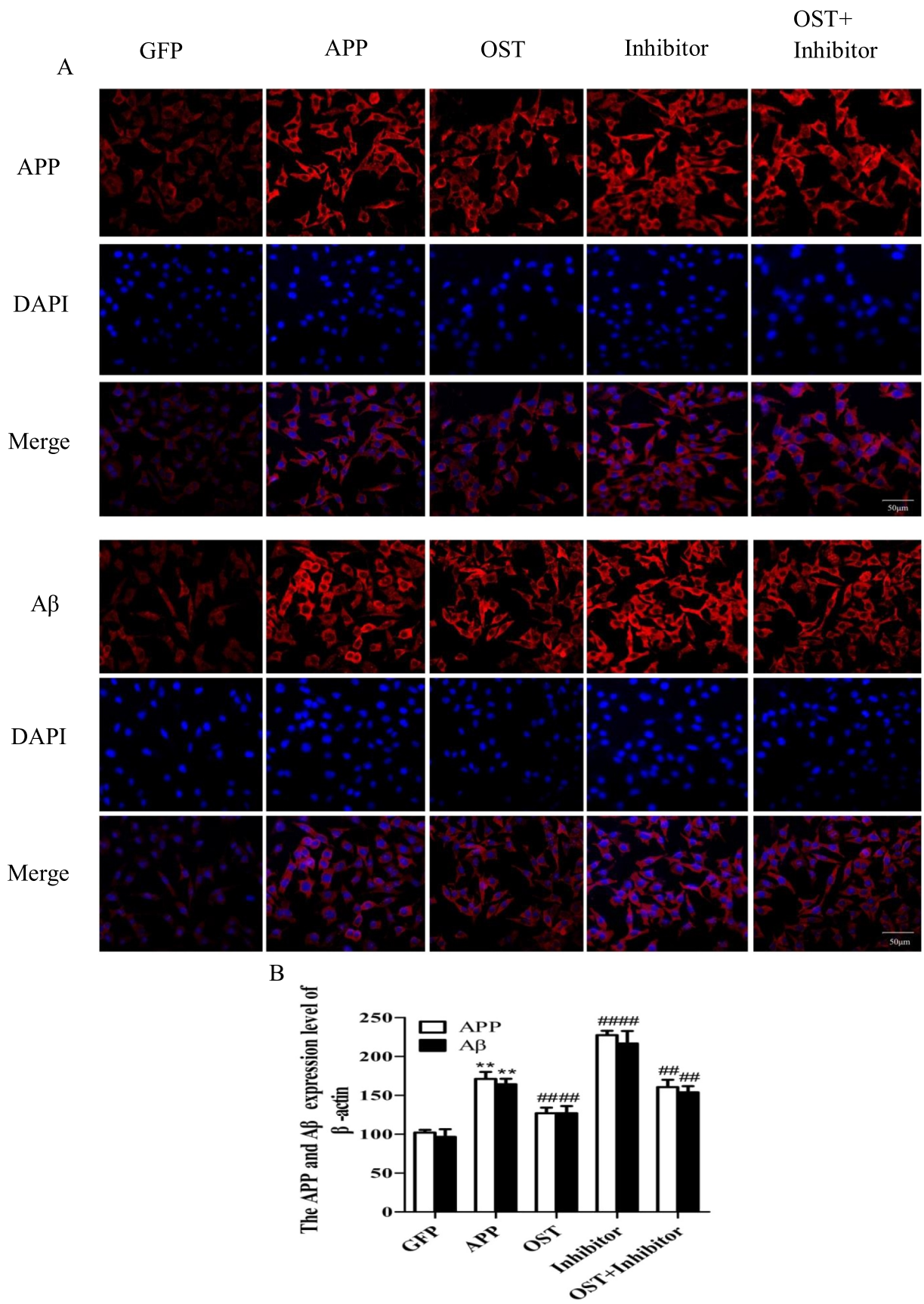


**Fig. 11.** Osthole suppresses the expression of APP, Aβ proteins in SH-SY5Y cells transduced APP.
(A) The immunofluorescence pictures of APP, Aβ;
(B) The expression of APP, Aβ proteins determined by ImageJ software.
$^{**}P < 0.01$ vs. GFP; $^{\#\#}P < 0.01$ vs. APP.

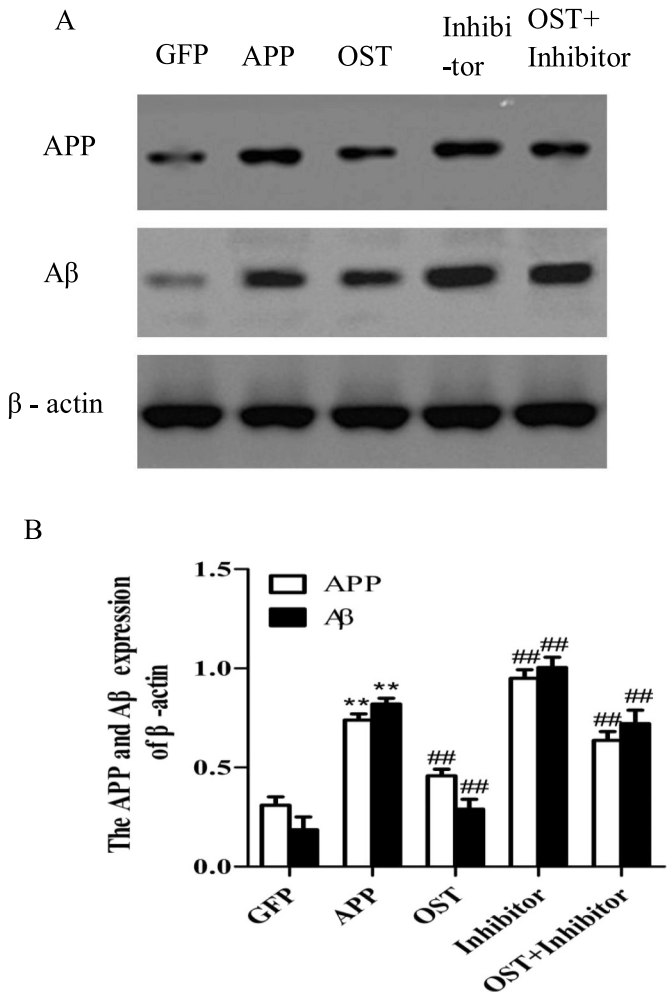


**Fig. 12.** The expression of APP and Aβ proteins with osthole treatment in cells. (A) The expression of APP and Aβ proteins were analyzed by Western blot; (B) The expression levels were semi-quantified by densitometric measurements, normalized with β-actin internal control. $n = 3$, $^{**}P < 0.01$ vs. GFP; $^{\#\#}p < 0.01$, $^{\#\#}P < 0.01$ vs. APP.

101a-3p was negatively correlated with the expression of APP mRNA and protein, there are negative correlation between miRNA-101a-3p and Aβ protein. So it can be say that the MiRNA-101a-3p inhibitor decrease the inhibitory effect of miR-101a-3p on the expression of Aβ protein in APP-SY5Y with overexpression of APP, and it was confirmed that osthole inhibited the expression of APP protein by up-regulating MiRNA-101a-3p.

## 4. Discussion

Alzheimer's disease (AD) is an APP-induced disease, which characterized by accumulation of senile plaques and the formation of neurofibrillary tangles in the brain [33]. The production and degradation of Aβ will be balance in normal, but in AD patient's brain, the amount of Aβ increased because of the aberrant expression of APP, Aβ plaque as the key factor of the formation and development of AD, produce neurotoxicity [34], and it activate a series of pathologies, which induces apoptosis in nerve cells.

Osthole as a natural coumarin compound is considered a therapeutic potential drug due to its broad pharmacological effects [35]. The pharmacological effects include anti-apoptosis [36], anti-oxidant [37] and neuroprotective effects. Previous studies in the laboratory found that osthole has neuroprotective effects on APP-SY5Y cells, and promotes the differentiation of neural stem into neurons by up-

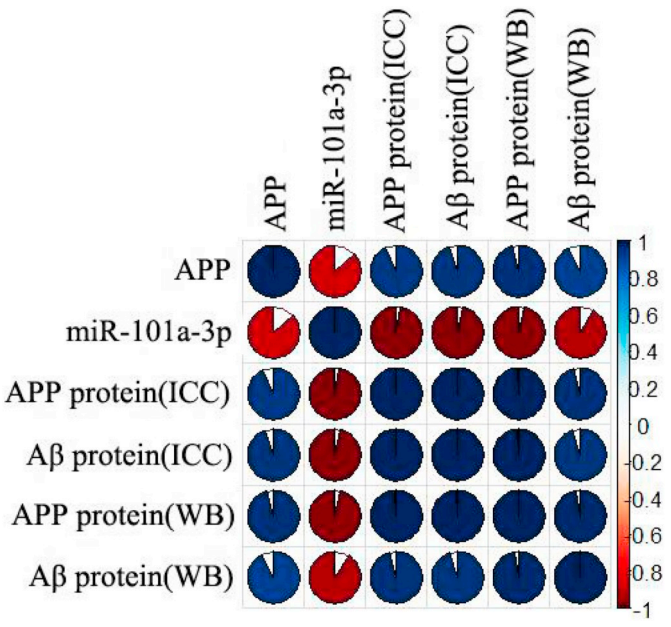


**Fig. 13.** The relationship of miRNA-101a-3p, APP and Aβ.
Red means the negative correlation; blue means positive correlation. (For interpretation of the references to color in this figure legend, the reader is referred to the web version of this article.)

regulating miR-9 [23] as well. MicroRNAs are abundant in the brain and participate in the development of AD. However, the miRNAs regulated by osthole in Alzheimer's disease is still a whitespace up to now.

Accumulated researches had verified that miRNA could affect various of disease. Among them, the microRNA related to Alzheimer's disease is a hot topic in Asia. MiR-298 [38], miR-384 [39], miR-124 [40], miR-9 [41] were determined to be a regulator of BACE-1, MiR-384 [39], miR-153 [42], miR-16 [43] were reported that it could affect the expression of APP in AD. MicroRNA-101 downregulates Alzheimer's amyloid-β precursor protein levels in human cell cultures and RanBP9 expression [44,45]. Liu D found that HDAC2/HNF-4A/miR-101b/AMPK Pathway could affect in development of AD [39]. So, it's meaningful to find the aberrant expression microRNA and the target mRNA regulated by microRNA in AD.

In this study, miRNA-101a-3p was selected as the differential miRNA which regulated by osthole in Alzheimer's disease. MiRNA-101a-3p bind to the 3′-UTR of APP was verified by the bioinformatics analysis, and then vilified by this biological experiment. APP/PS1 mice and SH-SY5Y cells with over-expression of APP were served as the AD model in vivo and in vitro. We found that osthole could increase the learning and memory ability of APP/PS1 mice and could increase the miRNA-101a-3p expression and reduce the levels of APP mRNA and protein at the same time. To observe the further study, miRNA-101a-3p inhibitor was used to explore whether osthole had the inhibitory effects to APP via up-regulating miRNA-101a-3p, RT-PCR was used to detect the expression of miRNA-101a-3p and APP mRNA, the results showed that osthole could decrease the expression of APP along with the increasing of miRNA-101a-3p. And the expression of APP and Aβ proteins were determined by western blot and ICC staining, these results indicated that the up-regulation of miRNA-101a-3p induced by osthole could inhibit the expression of APP to delay the occurrence of AD. The biological experiment verified the results from the microarray that miRNA-101a-3p was the osthole-mediated miRNA and the prediction from the bioinformatics that the miRNA-101a-3p could inhibit the expression of APP. But there is a new discovery in this study, with the increasing of APP, the levels of Aβ was raised at the same time. So, a question was posed that whether or not osthole had an effect on the

expression of BACE-1 through regulating miR-101a-3p.

In conclusion, above results indicated that APP mRNA and protein were over-expressed in Alzheimer's disease. MiRNA-101a-3p could bind to the 3′-UTR of APP to inhibit the APP expression in APP/PS1 mice and APP-SH-SY5Y cells. These findings indicated that miRNA-101a-3p could be used as the hall marker of AD.

## Disclosure statement

The authors declare that there is no conflict of interest associated with this study.

## Acknowledgments

The authors would like to thank Liaoning University of Traditional Chinese Medicine plant laboratory for the use of the microscope and freezing microtome.

## References

[1] A. Ochalek, B. Mihalik, H.X. Avci, et al., Neurons derived from sporadic Alzheimer's disease iPSCs reveal elevated TAU hyperphosphorylation, increased amyloid levels, and GSK3B activation[J], Alzheimers Res. Ther. 9 (1) (2017) 90, https://doi.org/10.1186/s13195-017-0317-z.

[2] D.C. Perry, J.A. Brown, K.L. Possin, et al., Clinicopathological correlations in behavioural variant frontotemporal dementia[J], Brain J. Neurol. 140 (12) (2017) 3329–3345, https://doi.org/10.1093/brain/awx254.

[3] J. Verheijen, Understanding Alzheimer disease at the interface between genetics and transcriptomics[J], Trends Genet. TIG 34 (6) (2018) 434–447, https://doi.org/10.1016/j.tig.2018.02.007.

[4] J. Dunys, A. Valverde, Are N- and C-terminally truncated Aβ species key pathological triggers in Alzheimer's disease?[J], J. Biol. Chem. (2018), https://doi.org/10.1074/jbc.R118.003999.

[5] T.J. Esparza, M. Gangolli, N.J. Cairns, Soluble amyloid-beta buffering by plaques in Alzheimer disease dementia versus high-pathology controls[J], PLoS One 13 (7) (2018) 0200251, , https://doi.org/10.1371/journal.pone.0200251.

[6] Y. Wang, T. Veremeyko, A.H. Wong, et al., Downregulation of miR-132/212 impairs S-nitrosylation balance and induces tau phosphorylation in Alzheimer's disease, Neurobiol. Aging 51 (2017) 156–166, https://doi.org/10.1016/j.neurobiolaging.2016.12.01-5.

[7] V. Chinchalongporn, M. Shukla, Melatonin ameliorates Aβ-induced alteration of βAPP-processing secretases via the melatonin receptor through the Pin1/GSK3β/NF-κB pathway in SH-SY5Y cells[J], J. Pineal Res. 64 (4) (2018) 12470, , https://doi.org/10.1111/jpi.12470.

[8] B. György, C. Lööv, M.P. Zaborowski, et al., CRISPR/Cas9 mediated disruption of the Swedish APP allele as a therapeutic approach for early-onset Alzheimer's disease [J], Mol. Ther. Nucleic Acids 11 (2018) 429–440, https://doi.org/10.1016/j.omtn.2018.03.007.

[9] J. Lee, A.A.S. Samson, Inkjet printing-based β-secretase fluorescence resonance energy transfer (FRET) assay for screening of potential β-secretase inhibitors of Alzheimer's disease[J], Anal. Chim. Acta 1022 (2018) 89–95, https://doi.org/10.1016/j.aca.2018.03.033.

[10] C. Sun, Y. Gui, R. Hu, et al., Preparation and pharmacokinetics evaluation of solid self-microemulsifying drug delivery system (S-SMEDDS) of osthole[J], AAPS PharmSciTech 19 (5) (2018) 2301–2310, https://doi.org/10.1208/s12249-018-1067-3.

[11] B. Wang, X. Zheng, J. Liu, et al., Osthole inhibits pancreatic cancer progression by directly exerting negative effects on cancer cells and attenuating tumor-infiltrating M2 macrophages[J], J. Pharmacol. Sci. 137 (3) (2018) 290–298, https://doi.org/10.1016/j.jphs.2018.07.007.

[12] D. Zhao, Q. Wang, Y. Zhao, et al., The naturally derived small compound osthole inhibits osteoclastogenesis to prevent ovariectomy-induced bone loss in mice[J], Menopause (New York, N.Y.) (2018), https://doi.org/10.1097/GME.0000000000011-50.

[13] M.R. Campos-Esparza, M.V. Sánchez-Gómez, C. Matute, Molecular mechanisms of neuroprotection by two natural antioxidant polyphenols, Cell Calcium 45 (2009) 358–368.

[14] L.X. Shen, L.Q. Jin, D.S. Zhang, Effect of osthol on memory impairment of mice in AlCl3-induced acute senile model[J], Yao Xue Xue Bao = Acta Pharmaceutica Sinica 37 (3) (2002) 178–180.

[15] X. Xu, X. Liu, Osthole inhibits gastric cancer cell proliferation through regulation of PI3K/AKT[J], PLoS One 13 (3) (2018) e0193449, , https://doi.org/10.1371/journal.pone.0193449.

[16] S. Davinelli, V. Calabrese, D. Zella, Epigenetic nutraceutical diets in Alzheimer's disease[J], J. Nutr. Health Aging 18 (9) (2014) 800–805, https://doi.org/10.1007/s12603-014-0520-6.

[17] Y.K. Hu, X. Wang, L. Li, et al., MicroRNA-98 induces an Alzheimer's disease-like disturbance by targeting insulin-like growth factor 1, Neurosci. Bull. 29 (2013) 745–751, https://doi.org/10.1007/s12264-013-1348-5.

[18] H.C. Zhu, L.M. Wang, M. Wang, et al., MicroRNA-195 downregulates Alzheimer's disease amyloid-β production by targeting BACE1[J], Brain Res. Bull. 88 (6) (2012) 596–601, https://doi.org/10.1016/j.brainresbull.2012.05.018.

[19] H. Che, L.H. Sun, F. Guo, et al., Expression of amyloid-associated miRNAs in both the forebrain cortex and hippocampus of middle-aged rat, Cell. Physiol. Biochem. 33 (2014) 11–22, https://doi.org/10.1159/000356646.

[20] S.S. Hébert, K. Horré, L. Nicolaï, et al., MicroRNA regulation of Alzheimer's amyloid precursor protein expression, Neurobiol. Dis. 33 (2009) 422–428, https://doi.org/10.1016/j.nbd.2008.11.009.

[21] Y. Jiao, L. Kong, Y. Yao, et al., Osthole decreases beta amyloid levels through up-regulation of miR-107 in Alzheimer's disease, Neuropharmacology 108 (2016) 332–344, https://doi.org/10.1016/j.neuropharm.2016.04.046.

[22] S. Li, Y. Yan, Y. Jiao, et al., Neuroprotective effect of osthole on neuron synapses in an Alzheimer's disease cell model via upregulation of microRNA-9, J. Mol. Neurosci. 60 (2016) 71–81, https://doi.org/10.1007/s12031-016-0793-9.

[23] S.H. Li, P. Gao, L.T. Wang, et al., Osthole stimulated neural stem cells differentiation into neurons in an Alzheimer's disease cell model via upregulation of microRNA-9 and rescued the functional impairment of hippocampal neurons in APP/PS1 transgenic mice, Front. Neurosci. 11 (2017) 340, https://doi.org/10.3389/fnins.2017.00340.

[24] L. Kong, Y. Hu, Y. Yao, et al., The coumarin derivative osthole stimulates adult neural stem cells, promotes neurogenesis in the hippocampus, and ameliorates cognitive impairment in APP/PS1 transgenic mice, Biol. Pharm. Bull. 38 (2015) 1290–1301, https://doi.org/10.1248/bpb.b15-00142.

[25] X.F. Dong, T. Wang, T. Li, et al., Expressions of synaptophysin and BDNF/Trk-B in cerebellum of APPswe/PS1dE9 transgenic mice, Zhongguo Ying Yong Sheng Li Xue Za Zhi 33 (2017) 488–492, https://doi.org/10.12047/j.cjap.5601.2017.116.

[26] Y. Pan, K. Omori, I. Ali, et al., Altered expression of small intestinal drug transporters and hepatic metabolic enzymes in a mouse model of familial Alzheimer's disease, Mol. Pharm. (2018), https://doi.org/10.1021/acs.molpharmaceut.8b00500.

[27] J.H. He, Z.P. Han, J.B. Zhou, et al., MiR-145 affected the circular RNA expression in prostate cancer LNCaP cells, J. Cell. Biochem. (2018), https://doi.org/10.1002/jcb.27181.

[28] F. Yang, X. You, T. Xu, et al., Screening and function analysis of microRNAs involved in exercise preconditioning-attenuating pathological cardiac hypertrophy, Int. Heart J. (2018), https://doi.org/10.1536/ihj.17-498.

[29] T. Muetze, Using the contextual hub analysis tool (CHAT) in cytoscape to identify contextually relevant network hubs, Curr. Protoc. Bioinformatics 59 (2017) 8.24.1–8.24.13, https://doi.org/10.1002/cpbi.35.

[30] Y. Yan, X. Ding, K. Li, B. Ciric, S. Wu, H. Xu, B. Gran, A. Rostami, G. Zhang, CNS-specific therapy for ongoing EAE by silencing IL-17 pathway in astrocytes, Mol. Ther. 20 (7) (2012) 1338–1348.

[31] Y. Yao, Z. Gao, W. Liang, L. Kong, Y. Jiao, S. Li, Z. Tao, Y. Hui, J. Yang, Osthole promotes neuronal differentiation and inhibits apoptosis via Wnt/β-catenin signaling in an Alzheimer's disease model, Toxicol. Appl. Pharmacol. 289 (3) (2015) 474–481.

[32] Y.H. Yan, S.H. Li, H.Y. Li, et al., Osthole protects bone marrow-derived neural stem cells from oxidative damage through PI3K/Akt-1 pathway, Neurochem. Res. 42 (2017) 398–405, https://doi.org/10.1007/s11064-016-2082-y.

[33] P.L. McGeer, NSAIDs and Alzheimer disease: epidemiological, animal model and clinical studies, Neurobiol. Aging 28 (2007) 639–647, https://doi.org/10.1016/j.neurobiolaging.2006.03.013.

[34] Y. Ling, K. Morgan, Amyloid precursor protein (APP) and the biology of proteolytic processing: relevance to Alzheimer's disease, Int. J. Biochem. Cell Biol. 35 (2003) 1505–1535.

[35] H.J. Ji, J.F. Hu, Y.H. Wang, et al., Osthole improves chronic cerebral hypoperfusion induced cognitive deficits and neuronal damage in hippocampus, Eur. J. Pharmacol. 636 (2010) 96–101, https://doi.org/10.1016/j.ejphar.2010.03.038.

[36] K. Li, D. Ding, Neuroprotection of osthole against cerebral ischemia/reperfusion injury through an anti-apoptotic pathway in rats, Biol. Pharm. Bull. 39 (2016) 336–342, https://doi.org/10.1248/bpb.b15-00699.

[37] K.F. Hua, S.M. Yang, T.Y. Kao, et al., Osthole mitigates progressive IgA nephropathy by inhibiting reactive oxygen species generation and NF-κB/NLRP3 pathway, PLoS One 8 (2013) e77794, , https://doi.org/10.1371/journal.pone.0077794.

[38] V. Boissonneault, I. Plante, S. Rivest, MicroRNA-298 and microRNA-328 regulate expression of mouse beta-amyloid precursor protein-converting enzyme 1[J], J. Biol. Chem. 284 (4) (2009) 1971–1981, https://doi.org/10.1074/jbc.M80753020-0.

[39] C.G. Liu, J.L. Wang, L. Li, MicroRNA-384 regulates both amyloid precursor protein and β-secretase expression and is a potential biomarker for Alzheimer's disease[J], Int. J. Mol. Med. 34 (1) (2014) 160–166, https://doi.org/10.3892/ijmm.2014.1780.

[40] X. Du, X. Huo, Y. Yang, et al., miR-124 downregulates BACE 1 and alters autophagy in APP/PS1 transgenic mice[J], Toxicol. Lett. 280 (2017) 195–205, https://doi.org/10.1016/j.toxlet.2017.08.082.
[41] H. Xie, Y. Zhao, Y. Zhou, et al., MiR-9 regulates the expression of BACE1 in dementia induced by chronic brain hypoperfusion in rats[J], Cell. Physiol. Biochem. Int. J. Exp. Cell. Physiol. Biochem. Pharmacol. 42 (3) (2017) 1213–1226, https://doi.org/10.1159/000478919.
[42] J.M. Long, B. Ray, MicroRNA-153 physiologically inhibits expression of amyloid-β precursor protein in cultured human fetal brain cells and is dysregulated in a subset of Alzheimer disease patients[J], J. Biol. Chem. 287 (37) (2012) 31298–31310, https://doi.org/10.1074/jbc.M112.366336.
[43] W. Liu, C. Liu, J. Zhu, et al., MicroRNA-16 targets amyloid precursor protein to potentially modulate Alzheimer's-associated pathogenesis in SAMP8 mice[J], Neurobiol. Aging 33 (3) (2012) 522–534, https://doi.org/10.1016/j.neurobiolaging.2010.04.034.
[44] C. Barbato, S. Pezzola, C. Caggiano, et al., A lentiviral sponge for miR-101 regulates RanBP9 expression and amyloid precursor protein metabolism in hippocampal neurons[J], Front. Cell. Neurosci. 8 (2014) 37, https://doi.org/10.3389/fncel.2014.00037.
[45] J.M. Long, MicroRNA-101 downregulates Alzheimer's amyloid-β precursor protein levels in human cell cultures and is differentially expressed[J], Biochem. Biophys. Res. Commun. 404 (4) (2011) 889–895, https://doi.org/10.1016/j.bbrc.2010.12.053.